Appl. Phys. B 70, 587–591 (2000) / Digital Object Identifier (DOI) 10.1007/s003409900156

Applied Physics B
Lasers
and Optics

Determination of nonlinear absorption and refraction by single Z-scan method

M. Yin[1,*], H.P. Li[2], S.H. Tang[1], W. Ji[1]

[1] Department of Physics, National University of Singapore, Singapore 119260
(Fax: +65/777-6126, E-mail: scip7193@nus.edu.sg)
[2] Photonics Laboratory, School of EEE, Nanyang Technological University, Singapore 639789

Received: 8 July 1999/Published online: 3 November 1999

Abstract. We report a simplified Z-scan technique based on a study on the symmetric features of a typical Z-scan curve. The contributions from the two-photon absorption (TPA) and the nonlinear refraction (NLR) are easily separated from a closed-aperture Z-scan curve using this method. And the determination of the two nonlinearities is simplified and unambiguous. We demonstrate this method on ZnSe, CdS, and ZnTe semiconductors with 120-fs laser pulses. And the influence from the uncertainty of the focal plane ($Z = 0$) position is discussed. It is also found that the TPA coefficient can be obtained independently without knowing the exact location of the focal point.

PACS: 42.65.An; 78.20.Ci; 78.40.Fy

Materials that possess third-order optical nonlinearities have been investigated extensively, for their application to high-speed all-optical switching devices [1]. To assess a material for the above application, one must characterize its index of non-linear refraction (NLR) and two-photon absorption (TPA) coefficient [2]. These two parameters may be determined by Z-scan technique [3], in which a sample is scanned near the focal region of a focused laser beam. As the sample is moved along the propagation direction of the laser beam, Z-axis, it consequently experiences a phase and intensity modulation, which can be observed on its transmittance measured as a function of the sample position (z). If all the transmitted light is measured, only TPA affects the Z-scan. In this case, it refers to as open-aperture Z-scan. If part of the transmitted light is detected due to the presence of an aperture in front of the detector, both NLR and TPA manifest themselves on a so-called closed-aperture Z-scan. To extract the NLR index, one must take the TPA value that is obtained from an open-aperture Z-scan, into the account in the closed-aperture Z-scan modeling [3].

In this paper, we present a general study on Z-scan curves measured with the aperture. We have found that, for laser beams with circular symmetry and low irradiances, the normalized transmittance $T(z)$ can be expressed by $1 + T_{\Delta\Phi}(z) + T_{\Delta\Psi}(z)$, where $T_{\Delta\Phi}(z)$ originating from NLR is an odd function of z; and $T_{\Delta\Psi}(z)$ caused by TPA is an even function of z. Consequently, $T_{\Delta\Phi}(z)$ and $T_{\Delta\Psi}(z)$ are easily separated from a closed-aperture Z-scan, $T(z)$, by the operations of $[T(z) - T(-z)]/2$ and $[T(z) + T(-z)]/2 - 1$, respectively. Thus, instead that both open- and closed-aperture Z-scans must be performed [3], one can obtain information on the NLR index (γ) and TPA coefficient (β) only from a single closed-aperture Z-scan. This simplified method is demonstrated on ZnSe, CdS, and ZnTe semiconductors. We also discuss possible sources for experimental errors in implementation and how to minimize these errors.

1 Theory

Consider a Z-scan experiment in which an incident laser beam with a circularly symmetric field is propagating along the z direction and is focused with a convex lens. On the lens plane perpendicular to the Z axis, the field is $E_0(r, t) = E_0(t)g_0(r)$, where $E_0(t)$, r, and $g_0(r)$ are the radiation electric field containing the temporal envelope of the laser pulses, the radial distance, and the normalized spatial profile of the beam, respectively. And $g_0(r)$ is assumed to be a real function. Under the Fresnel condition, the field $E_{\text{in}}(z, r, t)$ near the focal plane can be evaluated as [4],

$$\begin{aligned} E_{\text{in}}(z, r, t) &= E_{\text{i0}}(t)g(z, r) \\ &= \frac{E_0(t)}{\lambda f}\int_0^\infty 2\pi r' \mathrm{d}r' g_0(r')\, J_0\left(2\pi \frac{rr'}{f\lambda}\right) \\ &\quad \times \exp\left[-\mathrm{i}\pi \frac{z}{\lambda}\left(\frac{r'}{f}\right)^2\right], \end{aligned} \tag{1}$$

where $E_{\text{i0}}(t)$ is the on-axis electric field at focus, $g(z, r)$ the normalized spatial profile, f the focal length of the lens, λ the wavelength of the input beam, and J_0 the zeroth-order Bessel

*Corresponding author.

function. With the thin-sample approximation [3], the field $E_e(z, r, t)$ at the exit of the sample of thickness L and linear absorption coefficient α may be obtained as,

$$E_e(z, r, t) = E_{in}(z, r, t) \exp(-\alpha L/2) \times [1 + 2F(z, r)\Delta\Psi]^{i\frac{\Delta\Phi}{2\Delta\Psi} - \frac{1}{2}} , \quad (2)$$

where $F(z, r) = g(z, r)g^*(z, r)$, $\Delta\Phi = k\gamma I_0 f(t) L_{eff} = \Delta\Phi_0 f(t)$, $\Delta\Psi = \beta I_0 f(t) L_{eff}/2 = \Delta\Psi_0 f(t)$, $L_{eff} = [1 - \exp(-\alpha L)]/\alpha$, I_0 the on-axis irradiance of the laser beam at the focus, and $f(t)$ the irradiance temporal profile of the incident pulses. Considering the low-irradiance limit that $\Delta\Phi \ll 1$ and $\Delta\Psi \ll 1$, one can approximate $E_e(z, r, t)$ as,

$$E_e(z, r, t) = E_{e0}(t) g(z, r)[1 + iF\Delta\Phi - F\Delta\Psi] . \quad (3)$$

Based on the Huygens–Fresnel principle, the complex electric field at the detector plane $E_d(z, r, t)$ can be written in the form of operator H,

$$E_d(z, r, t) = CH[E_e] = E_{d0}(t)\{H[g] + iH[gF]\Delta\Phi - H[gF]\Delta\Psi\} , \quad (4)$$

where C is a constant and the operator H represents a Hankel-transform which is defined as,

$$H[G] = 2\pi \int_0^\infty r' dr' G(r', z) J_0(2\pi r' r) , \quad (5)$$

where $G(r', z)$ is an arbitrary function. Thus, the normalized transmittance is expressed as,

$$\begin{aligned} T(z) &= \frac{\int_{-\infty}^{\infty} dt \int_0^{ra} |E_d(z, r, t)|^2 r dr}{\int_{-\infty}^{\infty} dt \int_0^{ra} |E_d(\Delta\Phi = 0, \Delta\Psi = 0)|^2 r dr} \\ &= 1 + \frac{\int_{-\infty}^{\infty} |E_{d0}(t)|^2 f(t) dt \int_0^{ra} T_1 r dr}{\int_{-\infty}^{\infty} |E_{d0}(t)|^2 dt \int_0^{ra} T_0 r dr} \Delta\Phi_0 \\ &\quad + \frac{\int_{-\infty}^{\infty} |E_{d0}(t)|^2 f(t) dt \int_0^{ra} T_2 r dr}{\int_{-\infty}^{\infty} |E_{d0}(t)|^2 dt \int_0^{ra} T_0 r dr} \Delta\Psi_0 \\ &= 1 + T_{\Delta\Phi}(z) + T_{\Delta\Psi}(z) , \end{aligned} \quad (6)$$

where

$$T_0(z, r) = H[g(z, r)]H^*[g(z, r)] , \quad (7)$$

$$T_1(z, r) = i(H[gF]H^*[g] - H^*[gF]H[g]) , \quad (8)$$

and

$$T_2(z, r) = -(H[gF]H^*[g] + H^*[gF]H[g]) . \quad (9)$$

We notice that, because g_0 is assumed to be a real function, it is obvious that $g^*(z, r) = g(-z, r)$ and $[g(z, r)F(z, r)]^* = g(-z, r)F(-z, r)$. Therefore, $H[g]$ and $H[gF]$ present the same features,

$$H^*[g(z, r)] = H[g(-z, r)] , \quad (10)$$

$$H^*[g(z, r)F(z, r)] = H[g(-z, r)F(-z, r)] . \quad (11)$$

So, one can easily prove that, $T_0(-z, r) = T_0(z, r)$, $T_1(-z, r) = -T_1(z, r)$, $T_2(-z, r) = T_2(z, r)$. Since all the operations of integrals have no effect on the symmetry of z axis, we have,

$$T_{\Delta\Phi}(-z) = -T_{\Delta\Psi}(z) , \quad (12)$$

and

$$T_{\Delta\Psi}(-z) = T_{\Delta\Phi}(z) . \quad (13)$$

This shows us that we can conveniently obtain the two terms of transmittance due to NLR and NLA separately, by performing the operations,

$$T_{\Delta\Phi}(z) = [T(z) - T(-z)]/2 , \quad (14)$$

$$T_{\Delta\Psi}(z) = [T(z) + T(-z)]/2 - 1 . \quad (15)$$

By considering the on-axis Z-scan, and Gaussian beam in the low-irradiance limit, the two nonlinear terms in (6) can be expressed as,

$$T_{\Delta\Phi}(x) = \frac{4x}{(x^2 + 9)(x^2 + 1)} \Delta\Phi_0 , \quad (16)$$

$$T_{\Delta\Psi}(x) = -\frac{2(x^2 + 3)}{(x^2 + 9)(x^2 + 1)} \Delta\Psi_0 , \quad (17)$$

where $x = z/z_0$.

2 Experiment

To demonstrate the above method, we measured the nonlinearities in ZnSe, CdS, and ZnTe samples which are all 1 mm in thickness. These materials were chosen because their third-order nonlinear optical properties have been intensively studied [5–8], and also partially because they all show two-photon absorption with a mode-locked Ti: sapphire laser (Coherent, Mira 900) that delivered laser pulses of 120 fs duration at 780 nm wavelength. The laser was operated at a repetition rate of 76 MHz. The spatial profile of the laser beam was nearly Gaussian distribution after a spatial filter. The laser pulses were divided by a beam-splitter into two parts, the reflected one which was used as a reference representing the incident light, and the transmitted one which was focused through the sample. The minimum beam waist of the focused laser beam was 20 μm (HW1/e^2M). Both beams were recorded by two power probes (Newport 818 SL) simultaneously, and measured by a dual-channel power meter (Newport 2832-C) which transferred the digitized signals to a computer. The sample was mounted on a computer-controlled translation stage, and was able to move along the Z axis with respect to the focus of the lens. An aperture with its transmittance, $S = 0.07$, was placed in front of the transmission detector. Note that the value of S is so small that the on-axis transmittance is measured to meet the on-axis requirement in the theory described in previous section.

The experimental results for ZnSe are shown as Fig. 1a. It should pointed out that, on femtosecond time scales, free-carrier absorption and refraction play no important role on the measured nonlinearities [6]. In addition, the average power (49 mW) used is so small that thermal-lensing effect is esti-

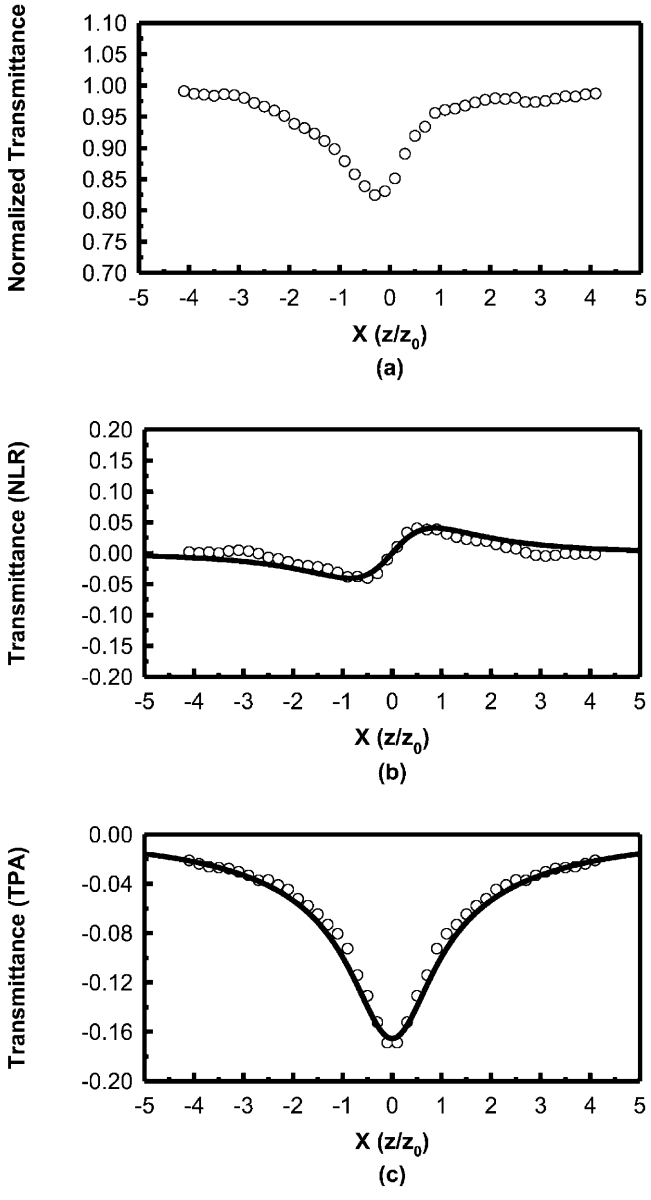

Fig. 1. **a** Closed-aperture Z-scan of 1-mm ZnSe with the 780-nm, 120-fs laser pulses. **b**,**c** Separated transmittance curves due to NLR and TPA, respectively. The *solid lines* are theoretical fits, where $\gamma = 2.4\times10^{-14}$ cm^2/W and $\beta = 3.6\times10^{-9}$ cm/W

mated to be negligible in our experiment. Therefore, Fig. 1a shows a resultant effect of both TPA and NLR of bound electronic nature. By applying operations (14) and (15), we separate the two nonlinearities, and display them in Figs. 1b and 1c, respectively. From Fig. 1c, we measure the deduction on the transmittance at the focus to be 0.17. Substituting $\alpha_0 = 0.19\,\text{cm}^{-1}$ and $I_0 = 1.34\,\text{GW/cm}^2$ into (17), we obtain $\beta = 3.6\times10^{-9}$ cm/W. Similarly, from Fig. 1b we measure the difference between the peak and valley on the transmittance to be 0.1. With (16), we derive $\gamma = 2.4\times10^{-14}$ cm^2/W (1.0×10^{-11} esu). The nonlinear indices of the other samples have been measured in the same way. The results are summarized in Table 1 and compared with the values calculated from the theoretical model of Sheik-Bahae et al. [9]. Our results are in good agreement with those obtained by standard Z-scan method [6].

Table 1. Measured two-photon absorption coefficients and nonlinear refractive indices for ZnSe, CdS, and ZnTe, with comparison to the theoretical values

Material	β /(cm/GW)			γ /(cm^2/W)		
	Exp.[a]	Exp.[b]	Theo.	Exp.[a]	Exp.[b]	Theo.
ZnSe	3.6	3.5	4.4	2.4×10^{-14}	2.5×10^{-14}	5.1×10^{-14}
CdS	4.9	6.4	4.3	3.6×10^{-14}	1.7×10^{-14}	2.7×10^{-14}
ZnTe	4.7	—	4.6	$<0.5\times10^{-14}$*	—	≈ 0

[a] This study.
[b] [6]
* This is the upper bound because the signal was below the sensitivity of the experiment

3 Discussion

It is well known that the minimum on the normalized transmittance of a closed-aperture Z-scan is displaced from the focal point [3]. The accurate location of the focal point is crucial in operations (16) and (17). To estimate the error caused by mistaking a displacement $\Delta x z_0$ away from the actual focal point in the operations, we derive that the total transmittance should be

$$T(x) = 1 + \frac{4(x+\Delta x)}{((x+\Delta x)^2+9)((x+\Delta x)^2+1)}\Delta\Phi_0 - \frac{2((x+\Delta x)^2+3)}{((x+\Delta x)^2+9)((x+\Delta x)^2+1)}\Delta\Psi_0\,. \tag{18}$$

Thus by the operating of (14) and (15), the results are not simply functions of NLR or TPA, but functions of both of them,

$$T_-(x) = \left(\frac{2(x+\Delta x)}{((x+\Delta x)^2+9)((x+\Delta x)^2+1)} - \frac{2(-x+\Delta x)}{((-x+\Delta x)^2+9)((-x+\Delta x)^2+1)}\right)\Delta\Phi_0 - \left(\frac{((x+\Delta x)^2+3)}{((x+\Delta x)^2+9)((x+\Delta x)^2+1)} - \frac{((-x+\Delta x)^2+3)}{((-x+\Delta x)^2+9)((-x+\Delta x)^2+1)}\right)\Delta\Psi_0\,, \tag{19}$$

$$T_+(x) = \left(\frac{2(x+\Delta x)}{((x+\Delta x)^2+9)((x+\Delta x)^2+1)} + \frac{2(-x+\Delta x)}{((-x+\Delta x)^2+9)((-x+\Delta x)^2+1)}\right)\Delta\Phi_0 - \left(\frac{((x+\Delta x)^2+3)}{((x+\Delta x)^2+9)((x+\Delta x)^2+1)} + \frac{((-x+\Delta x)^2+3)}{((-x+\Delta x)^2+9)((-x+\Delta x)^2+1)}\right)\Delta\Psi_0\,. \tag{20}$$

The numerical curves in Fig. 2 show that, when the location of the Z-axis origin has a deviation of no greater than $0.1z_0$ from the focus, the uncertainty of the transmittance will not

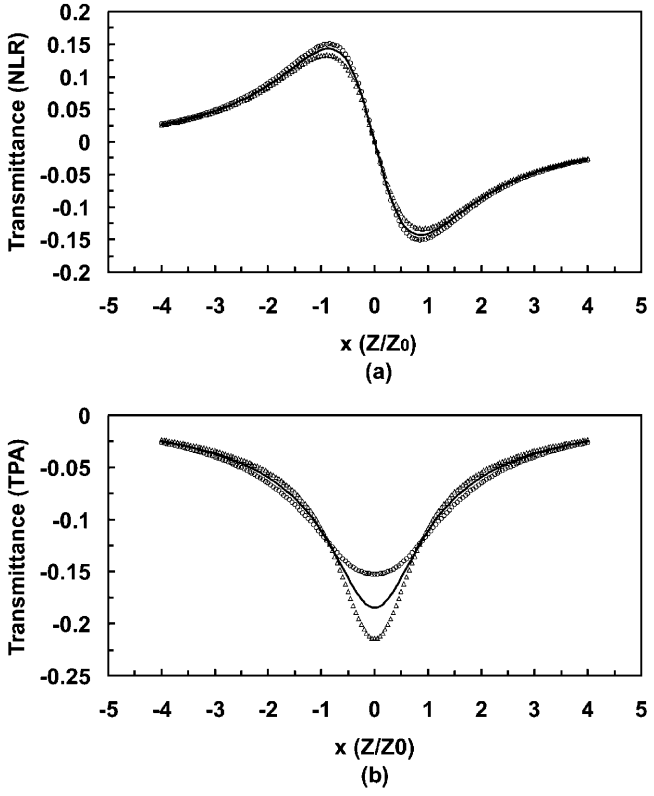

Fig. 2. On-axis Z-scans with dislocation $\Delta x = 0$ (*solid lines*); $\Delta x = -0.1$ (*circled curves*); and $\Delta x = 0.1$ (*triangled curves*). The Z-scans in **a** and **b** are caused by the NLR and TPA, respectively

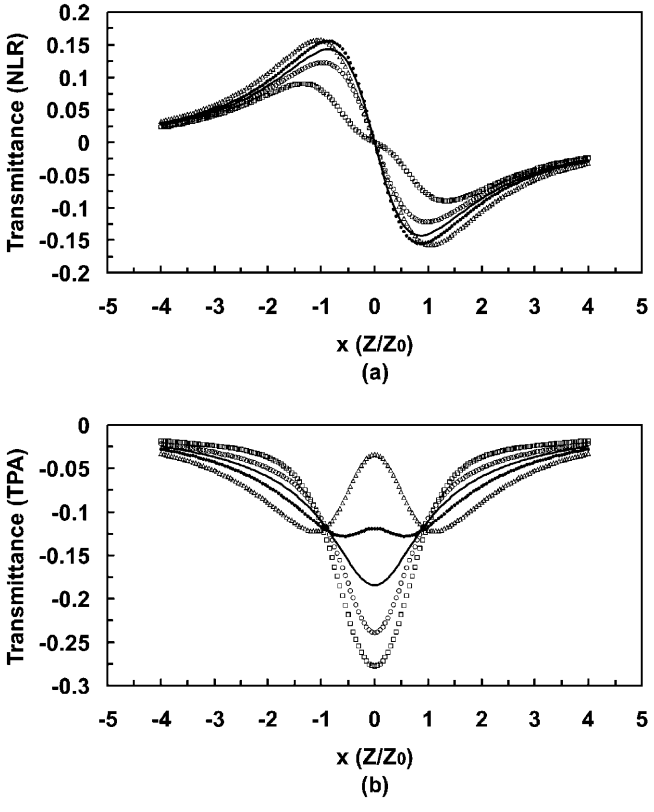

Fig. 3. On-axis Z-scans with $\Delta x = 0$ (*solid curves*); $\Delta x = -0.2$ (*dots*); $\Delta x = 0.2$ (*circles*); $\Delta x = -0.5$ (*triangles*); and $\Delta x = 0.5$ (*squares*). The Z-scans in **a** and **b** are caused by the NLR and TPA, respectively

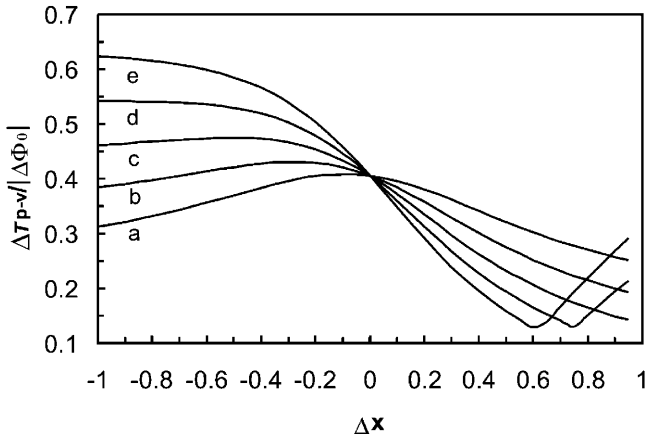

Fig. 4. Calculated dependence of $\Delta T_{\text{p-v}}/|\Delta\Phi_0|$ on the Δx, with $|\Delta\Psi_0/\Delta\Phi_0| = 0.1$ (a), 0.3 (b), 0.5 (c), 0.7 (d), and 0.9 (e), respectively

go beyond ±10%. In Fig. 3, also illustrated are the cases of $|\Delta x| = 0.2$ and 0.5 in which greater distortions appear on the Z-scan signals. The dependence of $\Delta T_{\text{p-v}}$ on the uncertainty of the focus is shown in Fig. 4, where $\Delta T_{\text{p-v}}$ is calculated as a function of Δx for $|\Delta\Psi_0/\Delta\Phi_0| = 0.1, 0.3, 0.5, 0.7$, and 0.9. Again it displays that when $\Delta x < 0.1$, the error is less than 10%.

To accurately measure the TPA coefficient, we carefully examine the numerical results in Fig. 2b and Fig. 3b. We note that, in all the curves, there are two points ($|x| = 0.858$) where the transmittances are nearly independent of Δx. This numerical result can be employed for the determination of the TPA coefficient. From these two points, the nonlinear absorption coefficient β can be unambiguously deduced, without consideration of the effect of Δx. At these two points the normalized transmittance can be expressed as,

$$T_+(x) = -\frac{4(3x^4+10x^2-9)\Delta x}{(x^2+9)^2(x^2+1)^2}\Delta\Phi_0 - \frac{2(x^2+3)}{(x^2+9)(x^2+1)}\Delta\Psi_0\,. \tag{21}$$

The first term is very close to zero at the two points. Hence (21) is almost the same as (17). With this fact, one can use this simple relation to calculate β as $T_{\Delta\Psi}(x = \pm 0.858) \approx -0.203\Delta\Psi_0$ for arbitrary values of Δx. This method is desirable because β can be determined without performing curve fitting to the experimental data. Yet the result is numerically calculated to be accurate to within 2% for Δx even as great as 0.2.

It should also be pointed out that our method could be very sensitive as a way to locate the focus of the laser beam. In conventional Z-scan experiments, an open-aperture measurement is always required to carry out in advance, not only to determine the TPA coefficient but also locate the origin of the z-coordinate. Our method, however, does not demand it. One can determine the Z-axis origin by the following procedure. (i) By operations of (14) and (15), the normalized closed-aperture Z-scan is separated into two curves for the NLR and TPA, respectively, with the estimated position of the focus. (ii) The first step is repeated with several shifts in the Z-axis origin used in the operations ($\Delta x = 0.0, \pm 0.2, \pm 0.4$, etc.). (iii) the two points ($x = \pm 0.858$) can be determined

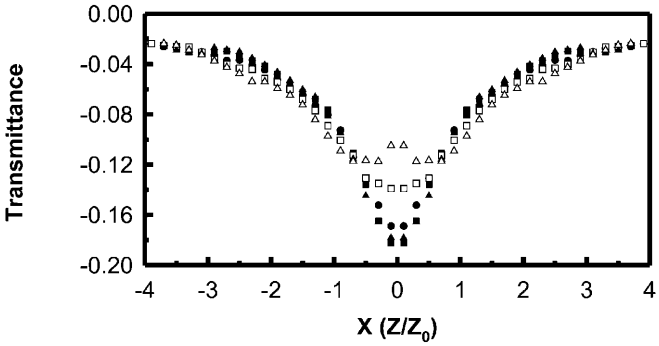

Fig. 5. Normalized transmittance due to TPA with various $\Delta x = 0$ (*dots*); $\Delta x = 0.2$ (*filled squares*); $\Delta x = -0.2$ (*open squares*); $\Delta x = 0.4$ (*filled triangles*); and $\Delta x = -0.4$ (*open triangles*), respectively. The five curves are very closely overlapped at the positions $x = \pm 0.85$

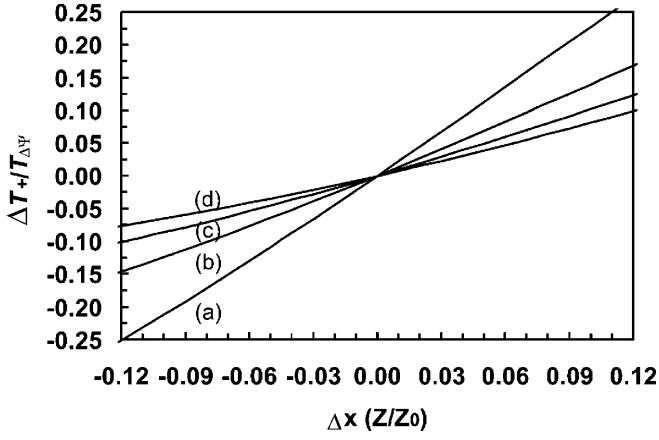

Fig. 6. Calculated $\Delta T_+(0)/T_{\Delta\Psi}(0)$ as a function of the dislocation of the focus (Δx) with $|\Delta\Psi_0/\Delta\Phi_0| = 0.3$ (a), 0.5 (b), 0.7 (c), and 0.9 (d), respectively. The sensitivity in the determination of the focus, which is inversely proportional to the slope of the curves, increases as $|\Delta\Psi_0/\Delta\Phi_0|$ increases

from the TPA curves and then the focus can be located. To demonstrate this procedure, we carry out operations (14) and (15) with $\Delta x = 0.0, \pm 0.2$, and ± 0.4 on the experimental data from Fig. 1, and display the results in Fig. 5, which clearly show the two distinctive positions with $x = \pm 0.858$ from the origin of the Z-axis.

In fact this is a very sensitive method to locate the focal point. We estimate that, with an error in the measured normalized transmittance T_+ as large as 1%, the uncertainty in finding the location of the focal point should be within $\pm 0.0149 \times |\Delta\Psi_0/\Delta\Phi_0| \times Z_0$. The dependence of $\Delta T_+(0)/T_{\Delta\Psi}(0)$ on the displacement of the focus is shown in Fig. 6 for various ratios of $|\Delta\Psi_0/\Delta\Phi_0|$, where $\Delta T_+(0)$ is defined as $\Delta T_+(0) = T_+(0) - T_{\Delta\Psi}(0)$. It illustrates that the larger the $|\Delta\Psi_0/\Delta\Phi_0|$ is, the more precisely the focus can be located.

4 Conclusion

We have studied the symmetric feature of the Z-scan curve, by which we demonstrate a simplified Z-scan method to measure the third-order optical nonlinearities. This method needs only a closed-aperture curve and a pair of simple operations to determine the nonlinear absorption coefficient and the nonlinear refractive index, respectively. The uncertainty of the measurement is $\pm 10\%$, and the location of $z = 0$ deviates no more than $0.1z_0$. A quick and reliable method to determine the TPA coefficient independently of the uncertainty of focus is also demonstrated, from which we can calibrate the focus of the laser beam accurately. This study also presents a valuable tool for other NLA-related Z-scans.

Acknowledgements. We gratefully acknowledge Dr. Li Yu for his valuable and informative discussions.

References

1. G.I. Stegman, E.M. Wright, N. Finlayson, R. Zanoni, C.T. Seaton: IEEE J. Light. Tech. **6**, 953 (1988)
2. V. Mizrahi, K.W. DeLong, G.I. Stegeman, M.A. Saifi, M.J. Andrejco: Opt. Lett. **14**, 1140 (1989)
3. M. Sheik-Bahae, A.A. Said, T.H. Wei, D.J. Hagan, E.W. Van Stryland: IEEE J. Quantum Electron. **QE-26**, 760 (1990)
4. M. Born, E. Wolf: *Principles of Optics*, 6th edn. (Pergamon, Oxford 1980) Sect. 8.8
5. J. Wang, M. Sheik-Bahae, A.A. Said, D.J. Hagan, E.W. Van Stryland: J. Opt. Soc. Am. B **11**, 1009 (1994)
6. T.D. Krauss, F.W. Wise: Appl. Phys. Lett. **65**, 1739 (1994)
7. X.J. Zhang, H. Fang, S.H. Tang, W. Ji: Appl. Phys. B **65**, 549 (1997)
8. A.A. Said, M. Sheik-Bahae, D.J. Hagan, T.H. Wei, J. Wang, J. Young, E.W. Van Stryland: J. Opt. Soc. Am. B **9**, 405 (1992)
9. M. Sheik-Bahae, D.C. Hutchings, D.J. Hagan, E.W. Van Stryland: IEEE J. Quantum Electron. **QE-27**, 1296 (1991)